Influence of Cell Membrane Wrapping on the Cell-Porous Silicon Nanoparticle Interactions

Fontana, Flavia

2020-09-09

Fontana , F , Lindstedt , H , Correia , A , Chiaro , J , Kari , O , Ndika , J , Alenius , H , Buck , J , Sieber , S , Mäkilä , E , Salonen , J , Urtti , A , Cerullo , V , Hirvonen , J & Santos , H A 2020 , ' Influence of Cell Membrane Wrapping on the Cell-Porous Silicon Nanoparticle Interactions ' , Advanced Healthcare Materials , vol. 9 , no. 17 , 2000529 . https://doi.org/10.1002/adhm.202000529

http://hdl.handle.net/10138/319515
https://doi.org/10.1002/adhm.202000529

ADVANCED HEALTHCARE MATERIALS
www.advhealthmat.de

Influence of Cell Membrane Wrapping on the Cell–Porous Silicon Nanoparticle Interactions

Flavia Fontana, Hanna Lindstedt, Alexandra Correia, Jacopo Chiaro, Otto K. Kari, Joseph Ndika, Harri Alenius, Jonas Buck, Sandro Sieber, Ermei Mäkilä, Jarno Salonen, Arto Urtti, Vincenzo Cerullo, Jouni T. Hirvonen, and Hélder A. Santos**

Abstract: Biohybrid nanosystems represent the cutting-edge research in biofunctionalization of micro- and nano-systems. Their physicochemical properties bring along advantages in the circulation time, camouflaging from the phagocytes, and novel antigens. This is partially a result of the qualitative differences in the protein corona, and the preferential targeting and uptake in homologous cells. However, the effect of the cell membrane on the cellular endocytosis mechanisms and time has not been fully evaluated yet. Here, the effect is assessed by quantitative flow cytometry analysis on the endocytosis of hydrophilic, negatively charged porous silicon nanoparticles and on their membrane-coated counterparts, in the presence of chemical inhibitors of different uptake pathways. Principal component analysis is used to analyze all the data and extrapolate patterns to highlight the cell-specific differences in the endocytosis mechanisms. Furthermore, the differences in the composition of static protein corona between naked and coated particles are investigated together with how these differences affect the interaction with human macrophages. Overall, the presence of the cell membrane only influences the speed and the entity of nanoparticles association with the cells, while there is no direct effect on the endocytosis pathways, composition of protein corona, or any reduction in macrophage-mediated uptake.

1. Introduction

Cell membrane-wrapped nanoparticles (NPs) are under investigation in multiple applications, from vaccines to drug delivery systems, detoxification systems, and as cues for proliferation and differentiation of cells.[1–3] Moreover, these biohybrid nanosystems present interesting properties, including prolonged circulation time, reduced uptake by the mononuclear phagocyte system, tissue- and inflammation-targeting properties.[4–7] These properties derive both from the molecules decorating the membrane surface, including carbohydrates (both as cell-specific antigenic signature and as sialic acid residues), by a specific lipidic composition in the membrane (important for the right orientation of the membrane), and by the different proteins constituting the in vivo protein corona and by their orientation.[8–11] To date, the cell membrane coating technique has been successfully applied to nanomaterials

Dr. F. Fontana, H. Lindstedt, A. Correia, Prof. J. T. Hirvonen, Prof. H. A. Santos
Drug Research Program
Division of Pharmaceutical Chemistry and Technology
Faculty of Pharmacy
University of Helsinki
Helsinki FI-00014, Finland
E-mail: flavia.fontana@helsinki.fi; helder.santos@helsinki.fi

J. Chiaro, O. K. Kari, Prof. A. Urtti, Prof. V. Cerullo
Drug Research Program
Division of Pharmaceutical Biosciences
Faculty of Pharmacy
University of Helsinki
Helsinki FI-00014, Finland

Dr. J. Ndika, Prof. H. Alenius
Human Microbiome Research
Faculty of Medicine
University of Helsinki
Helsinki FI-00014, Finland

Prof. H. Alenius
Institute of Environmental Medicine
Karolinska Institutet
Stockholm SE-17177, Sweden

J. Buck, Dr. S. Sieber
Department of Pharmaceutical Sciences
University of Basel
Basel 4056, Switzerland

E. Mäkilä, Prof. J. Salonen
Laboratory of Industrial Physics
Department of Physics and Astronomy
University of Turku
Turku FI-20014, Finland

Prof. V. Cerullo
Translational Immunology Program (TRIMM)
Digital Precision Cancer Flagship (iCAN)
University of Helsinki
Helsinki FI-00014, Finland

Prof. V. Cerullo, Prof. H. A. Santos
Helsinki Institute of Life Science (HiLIFE)
University of Helsinki
Helsinki FI-00014, Finland

The ORCID identification number(s) for the author(s) of this article can be found under https://doi.org/10.1002/adhm.202000529

DOI: 10.1002/adhm.202000529

different in composition, size, charge, and hydrophobicity, ranging from polymeric to gold, silica, porous silicon (PSi) particles, and to electrospun fibers.[1] One of the main factors influencing the successful encapsulation of the particles has been identified in the particles' surface charge that results in electrostatic interactions between the negatively charged membrane and the particles, producing aggregates.[12,13] However, other factors, including the hydrophobicity of the particles, play a role for an effective membrane encapsulation.[5,12,14]

Interactions between cells and NPs influence the uptake, as well as the final intracellular fate of the particle with important consequences on the therapeutic efficacy.[15,16] Size, composition, electrostatic properties, shape, and hydrophobicity are amongst the NP's properties determining differences in the interaction with the cells.[15,17,18] The endocytosis mechanisms employed by NPs depend primarily on the size of the particles and the presence of aggregates or agglomerates.[19] For example, receptor-mediated and non-mediated uptake of NPs usually exploits the clathrin- and caveolin-mediated pathways, while macropinocytosis allows the unspecific uptake of nanoparticles up to 500 nm.[16,19] However, recent works have proposed an increased uptake by micropinocytosis for organic and particularly biohybrid NPs.[20,21] Moreover, the internalization of NPs by the cells is influenced also by the composition of the protein corona.[22] The impact of the protein corona on the properties of biohybrid nanosystems has only recently been evaluated, highlighting qualitative differences in few key proteins and some quantitative differences in the percentage of known proteins between traditional and biohybrid particles.[8] Furthermore, the composition of the protein corona influences also the NPs interactions with phagocytes and a different corona composition may explain the reduced interaction of biohybrid NPs with phagocyes.[23,24] Nevertheless, the effect of the cell membrane coating on the NPs' uptake and protein corona composition has not been fully evaluated yet.

In recent years the use of zebrafish embryos has started to challenge the use of rodent models for the preliminary screening of formulations, enabling a cheaper and high-through put alternative.[25] This model has provided interesting data in the formulation of liposomes, but it has never been employed before to evaluate the circulation profile and interaction with phagocytes of biohybrid NPs.[26]

PSi micro/nano-particles have been extensively investigated for drug delivery in the treatment of cancer, diabetes, and cardiovascular diseases.[27–33] Moreover, the material itself presents immunomodulatory properties due to the surface modification, which render it an attractive candidate as nanovaccine platform for cancer immunotherapy or for autoimmune diseases.[2,12,34] The coating with cell membrane moieties can thereby improve the circulation time, slow the recognition by the cells of the mononuclear phagocyte system, and act as source of antigens and danger signals.

Here, we compared in different cell lines the endocytic mechanisms of conventional (negatively charged and hydrophilic PSi) and biohybrid NPs in presence of chemical compounds known to inhibit the endocytic pathways and analyzed the effect of the different inhibitors by principal component analysis (PCA). Moreover, we assessed the differences in the composition of static protein corona when the particles were exposed to human plasma. Unexpected findings in the type of proteins retained on the cell membrane coated particles prompted us to compare their uptake in human macrophages and to preliminary evaluate their blood circulation behavior in a Zebrafish model.[25,26]

Table 1. Size and zeta potential of TRITC-TOPSi particles and TRITC-TOPSi particles extruded with the cell membrane derived from different cancer cell lines. The results are presented as mean ± s.d. ($n \geq 3$).

Particles	Size [nm]	PdI	Zeta Potential [mV]
TRITC-TOPSi	191 ± 2	0.104 ± 0.021	−23.5 ± 0.7
TRITC-TOPSi@A549	183 ± 7	0.089 ± 0.016	−29.3 ± 1.4
TRITC-TOPSi@MCF-7	181 ± 9	0.094 ± 0.040	−24.8 ± 1.29
TRITC-TOPSi@MDA-MB-231	178 ± 2	0.057 ± 0.020	−26.6 ± 1.7
TRITC-TOPSi@PC3MM2	182 ± 1	0.085 ± 0.025	−25.5 ± 1.1

2. Results and Discussion

2.1. Physicochemical Characteristics and Cytocompatibility of Cancer Cell Membrane-Coated Particles

Biohybrid particles were prepared by loading thermally oxidized porous silicon (TOPSi) NPs with tetramethylrhodamine (TRITC), followed by the extrusion with membranes derived from different cell lines (A549, MCF-7, MDA-MB-231, and PC3MM2), representing examples of lung carcinoma, breast cancer, and prostate cancer. The physical properties of these systems were then evaluated by dynamic and electrophoretic light scattering. As presented in **Table 1**, the extrusion with cell membranes derived from different cell lines resulted in particles presenting similar size, polydispersity index (PdI) and zeta potential. This result was expected, considering the physicochemical characteristics of TOPSi particles (negatively charged, hydrophilic, and easily dispersible in aqueous solution) and the optimal core particle characteristics of a biohybrid nanosystem.[12,13]

The particles were then imaged by transmission electron microscopy (TEM) to confirm the membrane wrapping in all the samples. As shown in **Figure 1**, there was no influence of the origin of the cell membrane on the encapsulation process. On the contrary, the presence of the cell membrane was evident in comparison with a TEM image of naked TOPSi particles (Figure S1, Supporting Information). Figure S2 in the Supporting Information shows the general view of the NPs population for all the samples.

Then, after confirming similar properties for all the particles formulated from different cell types, the impact of a homologous cell membrane coating on the cytocompatibility of the systems was evaluated by measuring the intracellular ATP levels after 24 h of incubation with the NPs. As shown in **Figure 2**, the cytocompatibility of PSi NPs coated with cell membranes increased in all the cell lines tested. In particular, for MDA-MB-231 and PC3MM2 cells, the naked particles were highly cytocompatible up to 100 and 250 μg mL^{-1}, while the coated NPs display cell viability values comparable to the control

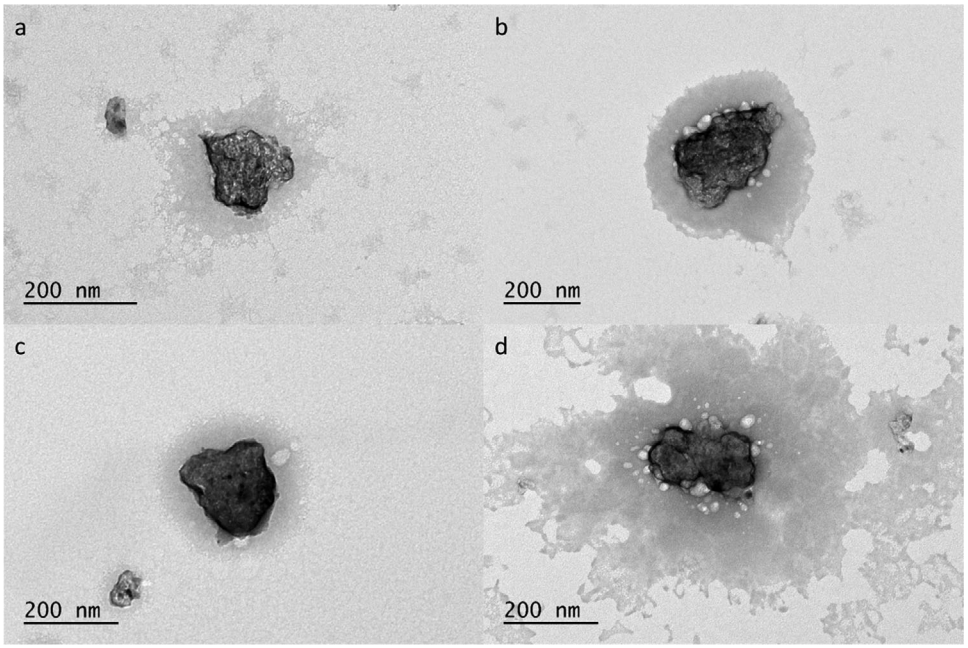

Figure 1. TEM images of a) TOPSi@A549, b) TOPSi@MCF-7, c) TOPSi@MBA-MD-231, and d) TOPSi@PC3MM2. The TEM grids containing the samples were negatively stained with uranyl acetate to highlight the presence of the cell membrane.

(Figure 2a) or to ≈50% of the control (Figure 2d) up to the highest concentration assessed. In the case of A549 and MCF-7 cells, TOPSi NPs presented an evident dose–response toxicity curve, which is shifted towards higher concentration when the NPs were coated with cell membrane (Figure 2b,c). The cytocompatibility profile of cell membrane-wrapped PSi NPs is in line with the results previously reported in other cells lines.[2,12] The concentration of 50 μg mL^{-1} was identified as non-toxic concentration to be used in the following studies.

2.2. Interactions between the NPs and the Cells

The endocytic mechanisms of naked and cell-membrane coated PSi NPs were first evaluated by flow cytometry (FCM) in presence of compounds inhibiting the uptake pathways. Before moving to the FCM experiment, we determined the IC_{50} of the compounds in all the cell lines (Figure S3, Supporting Information) after 4 h of incubation with the four different cancer cell lines. IC_{80} was also calculated and a concentration lower than the IC_{80} one was used in the following studies (concentrations reported in Table S1 in the Supporting Information). **Figure 3** shows the percentage of cells having NPs associated (A) or taken-up (U) after 1 or 3 h of incubation. In a previous work, we noticed that the presence of cancer cell membrane is increasing the uptake kinetic for oncolytic adenoviruses.[35] Thereby, the time-points of this experiments were chosen to evaluate any difference in the initial interaction between the coated or naked TOPSi NPs. The effects of the different parameters on the uptake of the NPs are summarized by the heatmap (Figure 3). TOPSi indicates the original particles, while TOPSi@CCM indicates particles coated with homologous cell membrane. As for the association of the particles with the cells, the map is divided horizontally into two big clusters, with the cluster on the right half of the heat-map clearly showing the higher percentage of association compared with the actual uptake, with higher percentage of positive cells for TOPSi 3 h association (T 3A), TOPSi 1 h association (T 1A), TOPSi@CCM 3 h association (TC 3A) and TOPSi@CCM 1 h association (TC 1A) compared to the same samples after fluorescence quenching with trypan blue (TOPSi 3 h uptake -T 3U-, TOPSi 1 h uptake -T 1U-, TOPSi@CCM 3 h uptake -TC 3U-, TOPSi@CCM 1 h uptake -TC 1U). Particularly, the presence of the cell membrane seemed to facilitate the association at earlier time point (1 h), as shown by the red and white colors in the column of TC 1A. Furthermore, the results suggested an independence of the association from the presence of the inhibitors of the endocytosis in solution (e.g., the data referring to chlorpromazine and 3-methyl-β-cyclodextrin in A549 and PC3MM2). Focusing on the uptake at +37 °C, MDA-MB-231 cells (37-231-MDA-MB-231) uptaked more NPs compared to the other cancer cell lines (in order from higher to lowest uptake, MDA-MB-231, PC3MM2, A549, and MCF-7), with a time-dependent increase in the fraction of positive cells. In particular, the presence of the homologous cell membrane increased the fraction of particles taken-up, when compared to the naked TOPSi NPs (TC 3U vs T 3U for MDA-MB-231). Previous experiments with particles coated with cell membrane derived from patient-derived xenografts hypothesized the presence of tumor proteins (like galectin-3 and carcinoembryonic antigens) that modulate the interaction with an homologous cancer cell.[36] Alternatively, the role of tumor associated carbohydrate antigens is still investigated as potential source for the enhanced interactions between homologous cell

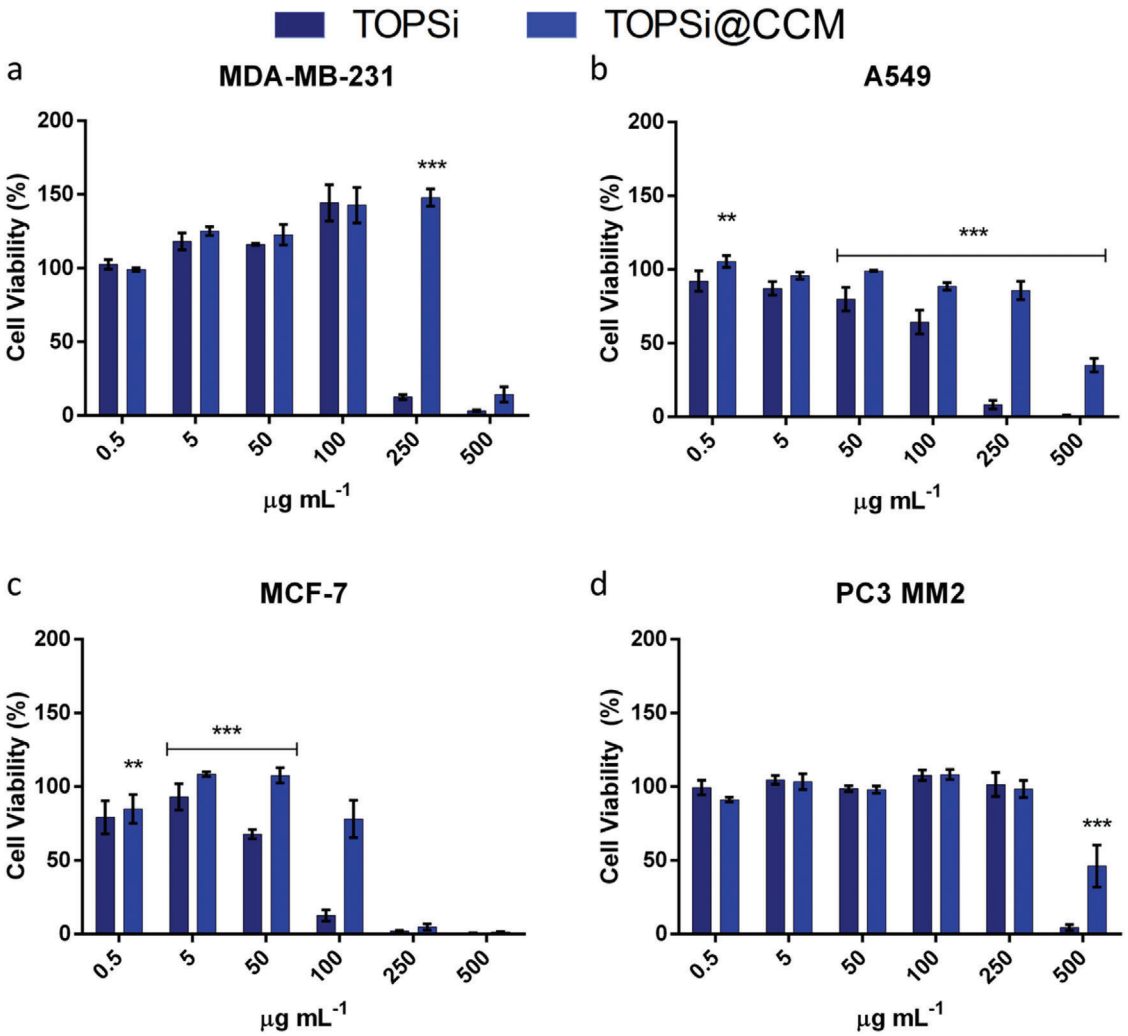

Figure 2. Cell viability (%) of a) MDA-MB-231, b) A549, c) MCF-7, and d) PC3 MM2 cancer cells after 24 h incubation with TOPSi or TOPSi wrapped with homologous cell membranes at different concentrations. Fetal bovine serum (10%) medium and Triton X-100 1% are the negative and positive controls, respectively. The results were normalized to the negative control and are presented as mean ± s.d. ($n = 4$). The data were analyzed with two-way ANOVA, followed by Bonferroni's post-test to evaluate the differences between coated and uncoated NPs. The levels of significance were set at the probabilities of $^{**}p < 0.01$ and $^{***}p < 0.001$.

membranes.[37] The endocytosis was greatly reduced for cells incubated in cold (all the samples marked with "ice"), identifying the need for energy in an active endocytosis, as suggested also by the size of the NPs.[38] The endocytic pathway of TOPSi NPs (columns T 3U and T 1U) appeared to be influenced by the presence of chlorpromazine, sucrose and 3-methyl-β-cyclodextrin, suggesting a clathrin mediated pathway. The presence of the cell membrane (columns TC 3U and TC 1U) increased the uptake in all the condition assessed, except for genistein, suggesting a role of caveolin and lipid rafts in the endocytosis and fusion of the membrane-enveloped particles.[39,40] Finally, the data showed a cell-dependent endocytotic profile of the particles, as previously demonstrated for other type of NPs.[40,41]

Then, to identify similarities and differences in the uptake profile of the nanosystems based on cell line and inhibitor of the uptake, we analysed the data presented in the heat-map by PCA (**Figure 4**). This kind of analysis has been used to identify similar clusters of data in different contexts.[42–45] Data were analysed by PCA using the Python Library Scikit-learn (the related code can be found as Python Jupiter Notebook as separate file in the Supporting Information). Figure 4a shows that the majority of the data identifying the different cells lines in presence of different inhibitors of the uptake clustered together highlighting few elements being outside the confidence ellipses, which identify the 68% (1σ) or 95% (2σ) of the values. The ellipses account for 1 or 2 standard deviations from the mean. The elements outside the confidence interval identified the cluster formed by the values of uptake of the NPs by 231 cells at +37 °C together with the lack of effect of chlorpromazine in A549 (first cluster from the top on the vertical clustering in the heatmap). As for chlorpromazine in PC3MM2 cells, these data were within the bigger cluster of data, which did not include 231 at +37 °C and chlorpromazine in

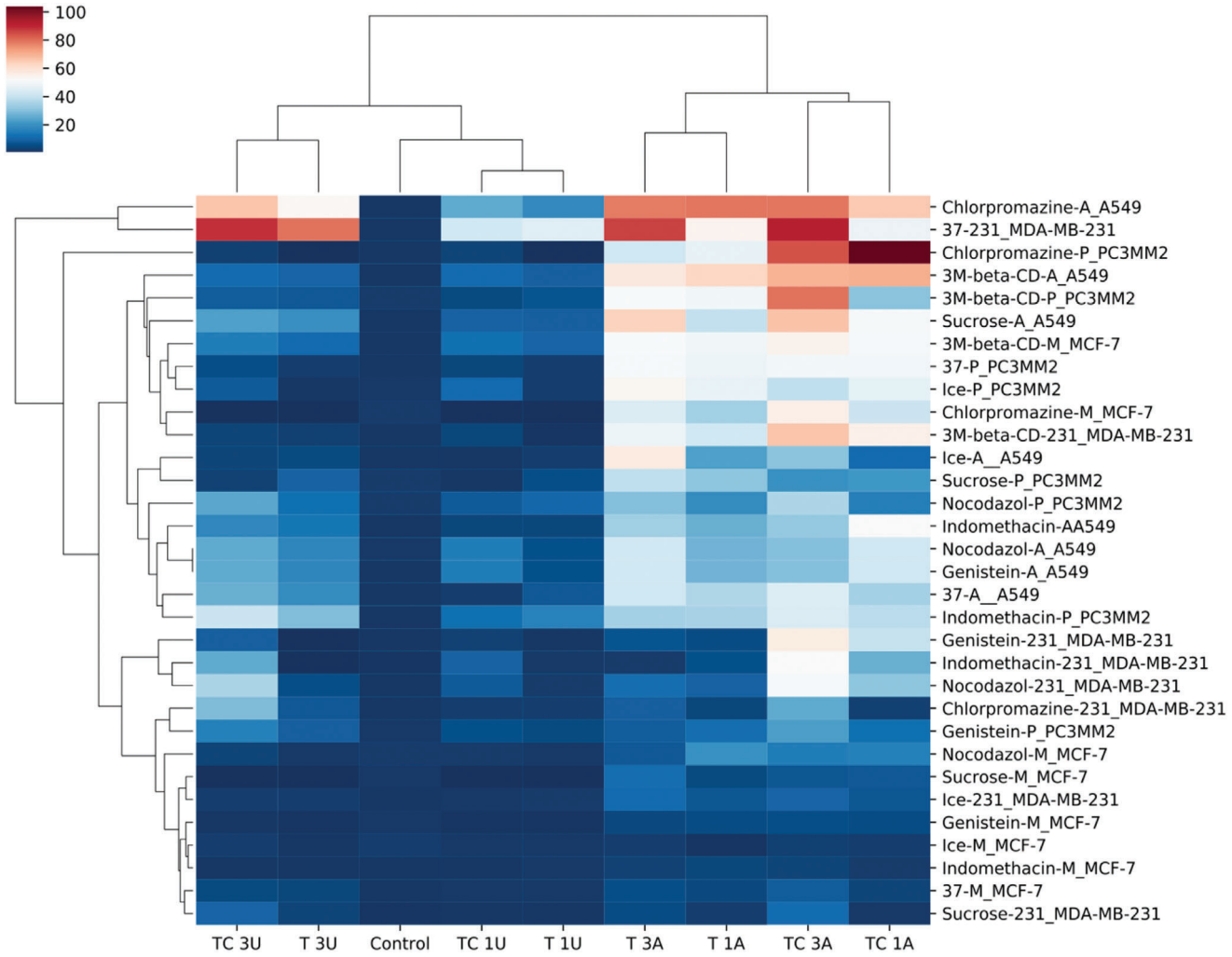

Figure 3. Heat-map displaying the mechanism of endocytosis of biohybrid nanoparticles. Cells (A549, A; MCF-7, M; MDA-MB-231, 231; PC3MM2, P) were incubated with different selective inhibitors of specific uptake mechanisms (i.e., ice, chlorpromazine, sucrose, indomethacin, nocodazol, genistein, and 3-methyl-β-cyclodextrin) and with fluorescently modified coated and uncoated particles (50 μg mL^{-1}) for 1 and 3 h. The samples were run into FCM to determine the fraction of particles associated before quenching the fluorescence with trypan blue and then run again in FCM. The results are presented as the mean of 3 samples (TC, TOPSi@CCM; T, TOPSi; A, Associated; U, Uptaken; 1, 1 h; 3, 3 h).

A549, but was separated from the other main cluster at the following node. Moreover, a second PCA, performed on the transposed dataset (evaluating the covariance of the type of particles, effect of quenching with trypan blue, and the incubation time), suggested that the cellular uptake was dependent on the interaction time and on the type of NP's surface, while the association was mainly influenced by the NP's surface (Figure 4b). These observations are based on the relative clustering of the different samples, with all the samples identified with U (uptake) clustering close to each other in PC1 and PC2 axis (except for TC 3U), while the samples identified with A clustered differently on PC2 axis depending of the incubation time, with a clear difference between naked and membrane-coated particles. The position of TC 3U in the plot suggested an effect of the surface coating with cell membrane on the uptake, while this effect was not seen at shorter time points (T 1 and TC 1 cluster together). Overall, the analysis of the data with heatmap and PCA suggests that the interactions between the cells and the particles is active and the uptake mechanism is cell-dependent, but generally clathrin-mediated with an influence of caveolin for the cell membrane-coated NPs.

In order to visually confirm the results obtained in FCM, the interaction between the NPs and the cells was imaged by confocal microscopy in the most interesting cases (A549 cells in selected conditions). Images of A549 cells incubated with the particles at +37 °C (Figure S4, Supporting Information) did not clearly present higher interaction for the cell membrane-coated NPs. Nevertheless, the interaction between the NPs and the cells was limited in the all the samples, due to the hydrophilic, negatively charged surface of the NPs, with only a mild effect of the cell membrane coating. The incubation with chlorpromazine reduced the interaction between the samples and the cells (as observed also in the quantitative analysis). As shown in Figure S5 in the Supporting Information, there was no effect of the cell membrane on the interaction between the cells and the NPs. The

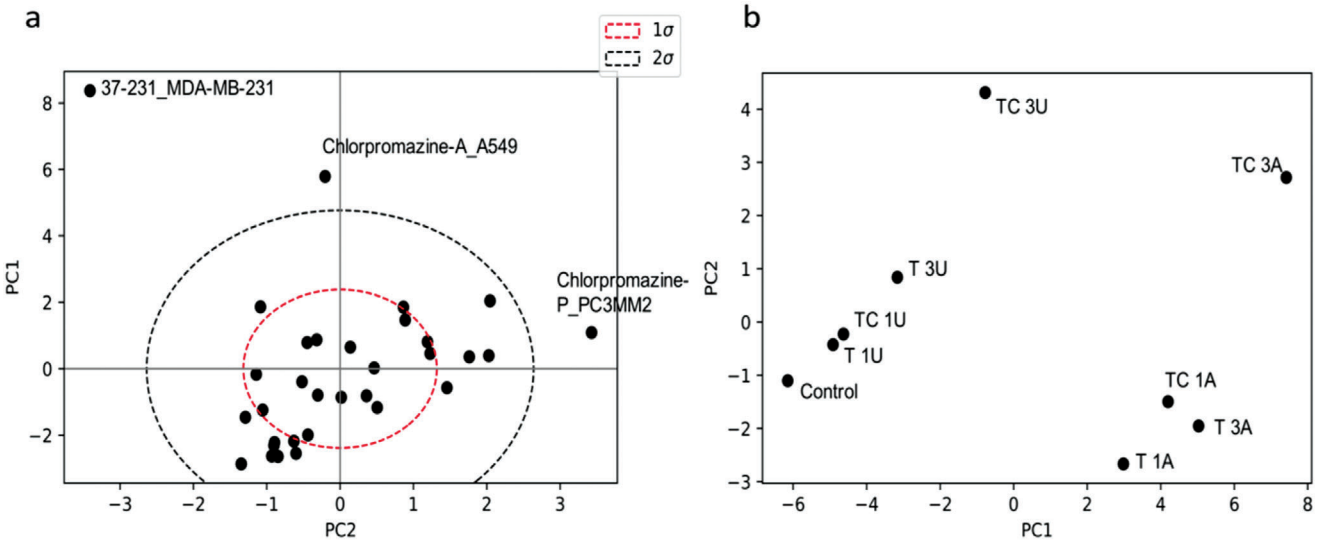

Figure 4. a) PCA of the effect of the coating with cell membrane on the uptake mechanisms of PSi NPs in different cells, in presence of uptake inhibitors. b) PCA of the transposed dataset to identify the effect of type of particle on association and uptake. The data were analyzed by PCA using Python Scikit-learn. The code can be found as separate Python Jupiter Notebook file in the Supporting Information.

confocal images of A549 cells incubated with sucrose confirmed the influence of the clathrin-mediated endocytosis mechanisms on the uptake of both TOPSi and membrane-coated NPs (Figure S6, Supporting Information). Finally, we also evaluated the uptake of the NPs in presence of 3-methyl-β-cyclodextrin (Figure S7, Supporting Information). The inhibition of the pinocytosis resulted in an inhibition of the NPs association with A549 cells. The presence of the cell membrane negatively influenced the association.

2.3. Protein Corona and Macrophage Uptake

One important variable interfering with the interactions between cell and NPs is the protein corona forming on the outer surface of the NPs upon immersion in a physiological fluid (e.g., plasma and extracellular matrix).[46] This phenomenon has been extensively investigated for different types of NPs over the years and for biohybrid vesicles (leukosomes),[8,22] but it has not been evaluated yet in presence of a biohybrid particle shielded with a layer of a cancer cell membrane. Some studies suggest that the prolonged circulation and stealth effect associated with cancer cell membrane-coated particles are associated with the cell membrane composition in lipids and proteins, with marginal focus on the circulatory or cytoplasmic protein coronas and their compositions.[47,48] Therefore, in this study we sought to evaluate the static protein corona after incubation in human plasma for 1 h (the "hard" corona) for both the naked and cancer cell membrane (A549)-coated NPs by mass spectrometry.

The Venn diagram presented in **Figure 5**a provides a visual summary of the qualitative protein corona composition. In particular, 88 proteins were found in all the samples, including the plasma supernatants. Naked and membrane-coated NPs shared additional 24 hits, with CCM-coated particles presenting 7 unique hits and TOPSi's corona presenting 18 unique hits. However, the heat-map in Figure 5b clearly depicts the differences in the corona composition between the two types of particles. From the results, it was possible to identify three bigger clusters of proteins: cluster 1 (whose composition is reported in Table S2 in the Supporting Information) was particularly enriched in the sample uncoated, with some few common proteins identified by cluster 4. On the contrary, cluster 2 was slightly positive for the CCM-coated particles and negative for the uncoated ones (composition in Table S4 in the Supporting Information) with cluster 3 (composition in Table S5 in the Supporting Information) highly positive for the CCM-particles and negative for TOPSi NPs alone. The hits identified in cluster 2 included some mRNA contaminants, together with complement factor H related protein, a component of the protein corona shown to prevent the activation of the complement. Cluster 3 contained proteins commonly expressed on the CCM or involved in cytoskeleton and membrane adhesion (e.g., cadherin 1 and myosin 9) with the complement component C8 gamma chain as protein corona component present only on CCM-coated NPs. The proteins identified within cluster 1 included the common constituents of hard protein corona in vitro, including fibrinogen, apolipoproteins, coagulation factors, thrombin and other proteins related with the coagulation.[49] In a previous study conducted on hydrophobic THCPSi NPs before and after modification with hydrophobin, THCPSi NPs did not bind to apolipoproteins before modification, contrary to the results with hydrophilic TOPSi.[50] The binding of fibrinogen and other coagulation factors has been correlated with uptake by neutrophils and their subsequent activation, with an inflammatory response.[51] Interestingly, the only differences amongst the particles (Table S2, Supporting Information) included proteins, like carboxypeptidase, commonly found in the protein corona surrounding silica particles.[52] These results were mirrored by the proteic composition of the supernatants, both in comparison with the relative NPs and between each other (Figures S8–S10, Supporting Information). Overall, as shown in Figure S11 in the Supporting Information, the majority of the proteins found in

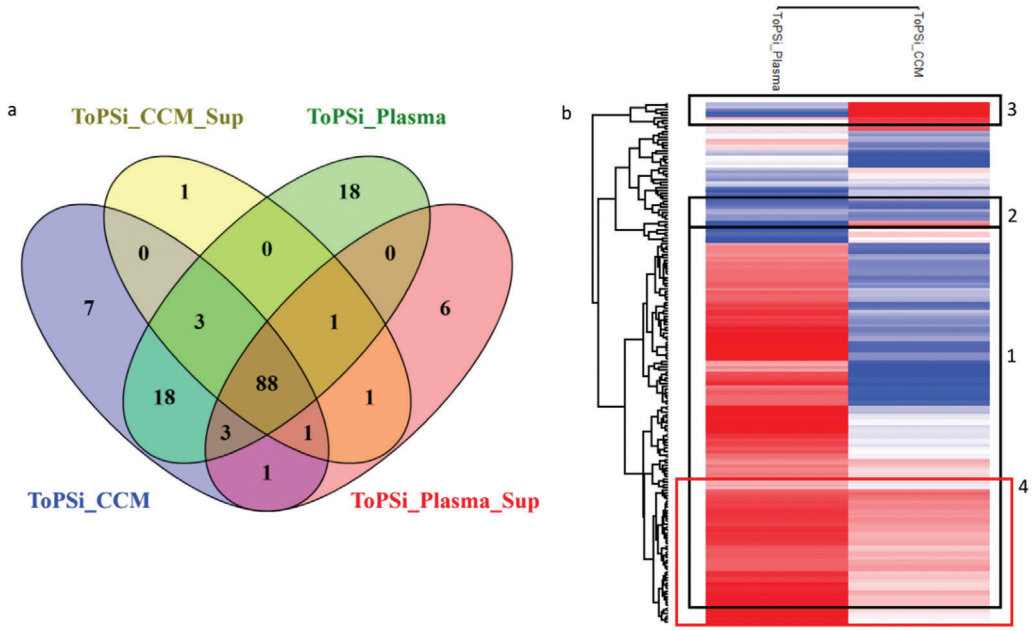

Figure 5. Mass spectrometry analysis of the composition of static protein corona. a) Venn diagram summarizing the total protein hits for each of the samples (TOPSi, TOPSi@CCM, and their respective plasma supernatants) and identifying the number of sample-exclusive or common hits. b) Heatmap illustrating the differences in the protein corona composition between naked (TOPSi) and membrane-coated (TOPSi@CCM) NPs. Red identifies positive events, while blue hits not found. The numbered squares correspond to the lists of identified proteins presented in the Supporting Information. The TOPSi@CCM NPs evaluated in this study were coated with A549 CCM.

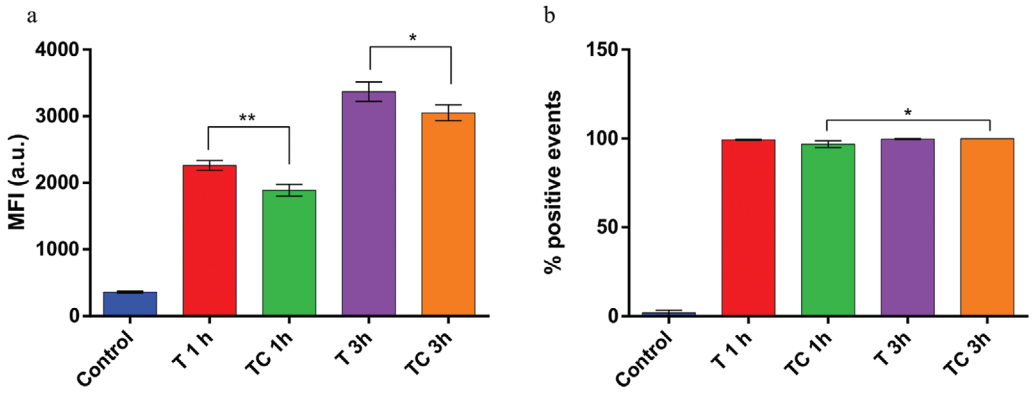

Figure 6. Interactions between KG-1 human macrophages and TOPSi (T) or TOPSi@A549 (TC), at the concentration of 50 μg mL^{-1}, after 1 or 3 h of incubations. The data are presented as mean ± s.d. ($n = 3$). The results were analyzed by one-way ANOVA followed by Tukey's multiple comparison. The levels of significance were set at the probability of $*p < 0.05$ and $**p < 0.01$.

the corona of the two particles are implicated in the activation of the complement or in interaction with lipids (like apolipoproteins). Thereby, the results suggest that there are no differences in the composition of the static protein corona in vitro which may justify the prolonged circulation of biohybrid NPs.

Based on the results from the protein corona analysis, we evaluated the interaction of A549 cell membrane-coated particles (TC) or TOPSi alone (T) by human macrophages. The mean fluorescent intensity (**Figure 6**a) confirmed the presence of a time-dependent interaction for both particles, despite the high percentage of positive events in all the samples (Figure 6b).

In different works, the interaction with the macrophages is evaluated cross species (murine macrophages with human cell membrane coating) or still displays interaction between particles and cells, though at lower extent compared to uncoated particles and liposome coated particles.[53,54] Moreover, the interaction is evaluated on adherent macrophages where the sedimentation of the nanosystems will contribute to their uptake. In this work, we evaluated the uptake by human macrophages in suspension, in conditions better mimicking the in vivo conditions. The results suggested an effect on the association for shorter time points (1 h), which however is reduced by increasing the incubation time (3 h). Nevertheless, the percentage of positive events was over 95% for all the samples, with non-significant or minimally significant differences amongst the samples.

These NPs were further injected into Zebrafish to evaluate their circulation profile and the interaction with macrophages in vivo. The preliminary results shown in Figure S12 in the

Supporting Information indicated that the NPs coated with CCM, independently from the source of the membrane, tended to aggregate more than the naked NPs. The aggregation played a role also in the enhanced interaction of CCM-coated particles with macrophages. Both at 1 and 24 h post-injection, the qualitative results suggested that biohybrid NPs displayed higher interaction with macrophages, as shown by bright agglomerates of NPs in the venous part of the zebrafish vasculature.[26] Further quantitative studies of interaction with the cells of the reticuloendothelial system and in vivo protein corona composition in murine models are needed to fully evaluate the contribution of CCM wrapping on the biodistribution of the nanosystems and their interaction with the cells of the innate immune system.

3. Conclusion

The effect of the cell membrane-layer on the interactions between negatively charged PSi NPs and cancer cell lines was evaluated in vitro. First, the wrapping of NPs with biohybrid cell membrane-derived moieties enhanced the cytocompatibility of the NPs in all the cell lines assessed. The association of the NPs to all the cell lines was improved when the NPs were coated with homologous cell membrane. This higher association of the NPs increased also the percentage of NPs taken-up after 3 h, when compared to the naked NPs. The endocytosis was proved to be cell line-dependent with different cell lines showing different susceptibility to the inhibition of specific pathways and not to be influenced by the type of cell membrane coating. Cell membrane-coated NPs were taken-up according to the same mechanisms of the naked NPs, with a major role played by clathrin-mediated endocytosis and micropinocytosis. The profile of the corona for both naked and cell membrane-coated particles was similar and resembled the profile of conventional NPs. Moreover, the presence of a cancer cell membrane wrapping had no effect on the percentage of positive events in human macrophages in suspension when compared to the naked NPs, while a lower interaction at shorter incubation points (1 h) could be observed from the analysis of the MFI. On the contrary, the coating with cell membrane increased the aggregation and the interaction with macrophages in a Zebrafish model, reducing the circulation time. However, the interaction of cancer cell membrane-coated NPs with cells of the innate immune system should be further evaluated in murine models for the mechanisms governing the enhanced homotopic accumulation in the tumors after intravenous injection, paying attention to different diseases models and animal characteristics (e.g., sex, age, weight), in order to have a more insightful indication of the potential of the biohybrid NPs in cancer therapy.

4. Experimental Section

The detailed description of the experiments performed in this work can be found from the Supporting Information.

Supporting Information

Supporting Information is available from the Wiley Online Library or from the author.

Acknowledgements

F.F. and O.K.K. acknowledge the Drug Research Program Joint Grant. S.S. is thankful for support of the "Stiftung zur Förderung des pharmazeutischen Nachwuchses in Basel" and the "Freiwillige Akademische Gesellschaft Basel." Zebrafish embryos were provided by the research group of Prof. M. Affolter at Biozentrum Basel. H.A.S. acknowledges financial support from the HiLIFE Research Funds, the Sigrid Jusélius Foundation, and the H2020 European Research Council Grant (Grant No. 825020). The authors also acknowledge the following core facilities funded by Biocenter Finland: Electron Microscopy Unit for TEM and the Light Microscopy Unit of the Institute of Biotechnology for the confocal microscope.

Conflict of Interest

The authors declare no conflict of interest.

Keywords

biohybrids, cancer cell membranes, nanoparticles, protein corona, nanoparticle uptake

Received: April 1, 2020
Revised: July 6, 2020
Published online:

[1] R. H. Fang, A. V. Kroll, W. Gao, L. Zhang, *Adv. Mater.* **2018**, *30*, 1706759.
[2] F. Fontana, M.-A. Shahbazi, D. Liu, H. Zhang, E. Mäkilä, J. Salonen, J. T. Hirvonen, H. A. Santos, *Adv. Mater.* **2017**, *29*, 1603239.
[3] R. H. Fang, C.-M. J. Hu, B. T. Luk, W. Gao, J. A. Copp, Y. Tai, D. E. O'connor, L. Zhang, *Nano Lett.* **2014**, *14*, 2181.
[4] R. Molinaro, C. Corbo, J. O. Martinez, F. Taraballi, M. Evangelopoulos, S. Minardi, I. K. Yazdi, P. Zhao, E. De Rosa, M. B. Sherman, A. De Vita, N. E. Toledano Furman, X. Wang, A. Parodi, E. Tasciotti, *Nat. Mater.* **2016**, *15*, 1037.
[5] A. Parodi, N. Quattrocchi, A. L. Van De Ven, C. Chiappini, M. Evangelopoulos, J. O. Martinez, B. S. Brown, S. Z. Khaled, I. K. Yazdi, M. V. Enzo, L. Isenhart, M. Ferrari, E. Tasciotti, *Nat. Nanotechnol.* **2013**, *8*, 61.
[6] C.-M. J. Hu, R. H. Fang, K.-C. Wang, B. T. Luk, S. Thamphiwatana, D. Dehaini, P. Nguyen, P. Angsantikul, C. H. Wen, A. V. Kroll, C. Carpenter, M. Ramesh, V. Qu, S. H. Patel, J. Zhu, W. Shi, F. M. Hofman, T. C. Chen, W. Gao, K. Zhang, S. Chien, L. Zhang, *Nature* **2015**, *526*, 118.
[7] L. Rao, L.-L. Bu, B. Cai, J.-H. Xu, A. Li, W.-F. Zhang, Z.-J. Sun, S.-S. Guo, W. Liu, T.-H. Wang, X.-Z. Zhao, *Adv. Mater.* **2016**, *28*, 3460.
[8] C. Corbo, R. Molinaro, F. Taraballi, N. E. Toledano Furman, K. A. Hartman, M. B. Sherman, E. De Rosa, D. K. Kirui, F. Salvatore, E. Tasciotti, *ACS Nano* **2017**, *11*, 3262.
[9] D. Walczyk, F. B. Bombelli, M. P. Monopoli, I. Lynch, K. A. Dawson, *J. Am. Chem. Soc.* **2010**, *132*, 5761.
[10] D. M. Beckwith, M. Cudic, *Semin. Immunol.* **2020**, *47*, 101389.
[11] X. Liang, X. Ye, C. Wang, C. Xing, Q. Miao, Z. Xie, X. Chen, X. Zhang, H. Zhang, L. Mei, *J. Controlled Release* **2019**, *296*, 150.
[12] F. Fontana, S. Albertini, A. Correia, M. Kemell, R. Lindgren, E. Mäkilä, J. Salonen, J. T. Hirvonen, F. Ferrari, H. A. Santos, *Adv. Funct. Mater.* **2018**, *28*, 1801355.
[13] B. T. Luk, C.-M. Jack Hu, R. H. Fang, D. Dehaini, C. Carpenter, W. Gao, L. Zhang, *Nanoscale* **2014**, *6*, 2730.
[14] R. Li, Y. He, S. Zhang, J. Qin, J. Wang, *Acta Pharm. Sin. B* **2018**, *8*, 14.

[15] S. Behzadi, V. Serpooshan, W. Tao, M. A. Hamaly, M. Y. Alkawareek, E. C. Dreaden, D. Brown, A. M. Alkilany, O. C. Farokhzad, M. Mahmoudi, *Chem. Soc. Rev.* **2017**, *46*, 4218.
[16] E. Polo, M. Collado, B. Pelaz, P. Del Pino, *ACS Nano* **2017**, *11*, 2397.
[17] L. Zhang, Q. Feng, J. Wang, S. Zhang, B. Ding, Y. Wei, M. Dong, J.-Y. Ryu, T.-Y. Yoon, X. Shi, J. Sun, X. Jiang, *ACS Nano* **2015**, *9*, 9912.
[18] R. Liu, W. Jiang, C. D. Walkey, W. C. W. Chan, Y. Cohen, *Nanoscale* **2015**, *7*, 9664.
[19] N. Oh, J. H. Park, *Int. J. Nanomed.* **2014**, 9 Suppl 1, 51
[20] T. K. Kaiser, M. Khorenko, A. Moussavi, M. Engelke, S. Boretius, C. Feldmann, H. M. Reichardt, *J. Controlled Release* **2020**, *319*, 360.
[21] S. Zhou, Y. Huang, Y. Chen, S. Liu, M. Xu, T. Jiang, Q. Song, G. Jiang, X. Gu, X. Gao, J. Chen, *Biomaterials* **2020**, *235*, 119795.
[22] C. Corbo, R. Molinaro, A. Parodi, N. E. Toledano Furman, F. Salvatore, E. Tasciotti, *Nanomedicine* **2016**, *11*, 81.
[23] V. Mirshafiee, R. Kim, S. Park, M. Mahmoudi, M. L. Kraft, *Biomaterials* **2016**, *75*, 295.
[24] H. Wang, Y. Liu, R. He, D. Xu, J. Zang, N. Weeranoppanant, H. Dong, Y. Li, *Biomater. Sci.* **2020**, *8*, 552.
[25] S. Sieber, P. Grossen, J. Bussmann, F. Campbell, A. Kros, D. Witzigmann, J. Huwyler, *Adv. Drug Delivery Rev.* **2019**, *151*, 152.
[26] S. Sieber, P. Grossen, P. Uhl, P. Detampel, W. Mier, D. Witzigmann, J. Huwyler, *Nanomed. Nanotechnol.* **2019**, *17*, 82.
[27] J. P. Martins, D. Liu, F. Fontana, M. P. A. Ferreira, A. Correia, S. Valentino, M. Kemell, K. Moslova, E. Mäkilä, J. Salonen, J. Hirvonen, B. Sarmento, H. A. Santos, *ACS Appl. Mater. Interfaces* **2018**, *10*, 44354.
[28] J. P. Martins, R. D'auria, D. Liu, F. Fontana, M. P. A. Ferreira, A. Correia, M. Kemell, K. Moslova, E. Mäkilä, J. Salonen, L. Casettari, J. Hirvonen, B. Sarmento, H. A. Santos, *Small* **2018**, *14*, 1800462.
[29] W. Li, Z. Liu, F. Fontana, Y. Ding, D. Liu, J. T. Hirvonen, H. A. Santos, *Adv. Mater.* **2018**, *30*, 1703740.
[30] F. Araújo, N. Shrestha, M. J. Gomes, B. Herranz-Blanco, D. Liu, J. J. Hirvonen, P. L. Granja, H. A. Santos, B. Sarmento, *Nanoscale* **2016**, *8*, 10706.
[31] M. P. A. Ferreira, S. Ranjan, A. M. R. Correia, E. M. Mäkilä, S. M. Kinnunen, H. Zhang, M.-A. Shahbazi, P. V. Almeida, J. J. Salonen, H. J. Ruskoaho, A. J. Airaksinen, J. T. Hirvonen, H. A. Santos, *Biomaterials* **2016**, *94*, 93.
[32] A. Correia, M.-A. Shahbazi, E. Mäkilä, S. Almeida, J. Salonen, J. Hirvonen, H. A. Santos, *ACS Appl. Mater. Interfaces* **2015**, *7*, 23197.
[33] J. Wolfram, H. Shen, M. Ferrari, *J. Controlled Release* **2015**, *219*, 406.
[34] M.-A. Shahbazi, T. D. Fernández, E. M. Mäkilä, X. Le Guével, C. Mayorga, M. H. Kaasalainen, J. J. Salonen, J. T. Hirvonen, H. A. Santos, *Biomaterials* **2014**, *35*, 9224.
[35] M. Fusciello, F. Fontana, S. Tähtinen, C. Capasso, S. Feola, B. Martins, J. Chiaro, K. Peltonen, L. Ylösmäki, E. Ylösmäki, F. Hamdan, O. K. Kari, J. Ndika, H. Alenius, A. Urtti, J. T. Hirvonen, H. A. Santos, V. Cerullo, *Nat. Commun.* **2019**, *10*, 5747.
[36] L. Rao, G.-T. Yu, Q.-F. Meng, L.-L. Bu, R. Tian, L.-S. Lin, H. Deng, W. Yang, M. Zan, J. Ding, A. Li, H. Xiao, Z.-J. Sun, W. Liu, X. Chen, *Adv. Funct. Mater.* **2019**, *29*, 1905671.
[37] L. Cai, Z. Gu, J. Zhong, D. Wen, G. Chen, L. He, J. Wu, Z. Gu, *Drug Discovery Today* **2018**, *23*, 1126.
[38] Y. Jiang, S. Huo, T. Mizuhara, R. Das, Y.-W. Lee, S. Hou, D. F. Moyano, B. Duncan, X.-J. Liang, V. M. Rotello, *ACS Nano* **2015**, *9*, 9986.
[39] Z. Luo, K. Cai, Y. Hu, B. Zhang, D. Xu, *Adv. Healthcare Mater.* **2012**, *1*, 321.
[40] T. Dos Santos, J. Varela, I. Lynch, A. Salvati, K. A. Dawson, *PLoS One* **2011**, *6*, 24438.
[41] D. A. Kuhn, D. Vanhecke, B. Michen, F. Blank, P. Gehr, A. Petri-Fink, B. Rothen-Rutishauser, *Beilstein J. Nanotechnol.* **2014**, *5*, 1625.
[42] J. R. Heath, A. Ribas, P. S. Mischel, *Nat. Rev. Drug Discovery* **2016**, *15*, 204.
[43] I. T. Jolliffe, J. Cadima, *Philos. Trans. R. Soc., A* **2016**, *374*, 20150202.
[44] C. Meng, O. A. Zeleznik, G. G. Thallinger, B. Kuster, A. M. Gholami, A. C. Culhane, *Briefings Bioinf.* **2016**, *17*, 628.
[45] J. Lever, M. Krzywinski, N. Altman, *Nat. Methods* **2017**, *14*, 641.
[46] G. Caracciolo, O. C. Farokhzad, M. Mahmoudi, *Trends Biotechnol.* **2017**, *35*, 257.
[47] H. Li, K. Jin, M. Luo, X. Wang, X. Zhu, X. Liu, T. Jiang, Q. Zhang, S. Wang, Z. Pang, *Cells* **2019**, *8*, 881.
[48] D. Nie, Z. Dai, J. Li, Y. Yang, Z. Xi, J. Wang, W. Zhang, K. Qian, S. Guo, C. Zhu, R. Wang, Y. Li, M. Yu, X. Zhang, X. Shi, Y. Gan, *Nano Lett.* **2020**, *20*, 936.
[49] A. Amici, G. Caracciolo, L. Digiacomo, V. Gambini, C. Marchini, M. Tilio, A. L. Capriotti, V. Colapicchioni, R. Matassa, G. Familiari, S. Palchetti, D. Pozzi, M. Mahmoudi, A. Laganà, *RSC Adv.* **2017**, *7*, 1137.
[50] M. Sarparanta, L. M. Bimbo, J. Rytkönen, E. Mäkilä, T. J. Laaksonen, P. Laaksonen, M. Nyman, J. Salonen, M. B. Linder, J. Hirvonen, H. A. Santos, A. J. Airaksinen, *Mol. Pharmaceutics* **2012**, *9*, 654.
[51] S. Keshavan, P. Calligari, L. Stella, L. Fusco, L. G. Delogu, B. Fadeel, *Cell Death Dis.* **2019**, *10*, 569.
[52] A. Solorio-Rodríguez, V. Escamilla-Rivera, M. Uribe-Ramírez, A. Chagolla, R. Winkler, C. M. García-Cuellar, A. De Vizcaya-Ruiz, *Nanoscale* **2017**, *9*, 13651.
[53] Q. Feng, X. Yang, Y. Hao, N. Wang, X. Feng, L. Hou, Z. Zhang, *ACS Appl. Mater. Interfaces* **2019**, *11*, 32729.
[54] H. Sun, J. Su, Q. Meng, Q. Yin, L. Chen, W. Gu, P. Zhang, Z. Zhang, H. Yu, S. Wang, Y. Li, *Adv. Mater.* **2016**, *28*, 9581.